Global Science Press

Optical and electronic properties of organoboron compounds in solvent

Yong Ding,[a, *], Rui Li,[a] Yue Gao,[a] Jing Shan[a,*]

Abstract. Organoboron compounds 1-4 with an aryl ring directly bound to a (FMes)$_2$B group through B-C bonds in vacuum, Hexane, Toluene, THF, CH$_3$CN were theoretically studied using DFT with B3LYP functional and 6-31G (d) basis set, and TD-DFT with CAM-B3LYP functional and 6-31G (d) basis set. The absorption and fluorescence spectra of compounds 1-4 are determined in the same and different solvents. It is found that the electronic transition is the most efficient when compounds 1-4 are in CH$_3$CN, the most polar solvent. The spectral contrast of compounds 3 and 4 is studied under different conditions. The charge difference density (CDD) is determined using the data from the intramolecular charge transfer of compounds 1-4 using 3D cube with large oscillator strength.

1. Introduction

Organoboron compounds have attracted considerable research interest in recent years due to their unique optoelectronic properties. It has been demonstrated that this kind of material can be used in a range of fields, such as nonlinear optics (NLO) [1-4], two-photon absorption (TPA) and emission materials [5-9], electron-transporting and emissive materials in organic light-emitting teleportation materials as well as chemosensors.

As early as 1955, Wittig and Herwig reported the photophysical properties of organoboron compounds [10], but it didn`t attract the attention of people because of their instability in air. In 1972 Williams demonstrated that the organoboron compounds become stable in air when two 1,3,5-trimethyl groups are added [11]. In order to improve the electron injecting and transporting properties in OLEDs, lower energy emission, and larger two-photon absorption cross sections and so on, many research groups looked for suitable organoboron compounds. However, most of these do not give sufficient steric protection to the boron centre to render it stable in air [12-16]. Marder et al. prepared three compounds using phenyl (1), 4-(1,1-Dimethylethyl) phenol (2) and 4-N,N-diphenylaminophenyl (3) groups attached to bis(fluoromesityl)boryl ((FMes)2B) by B – C bonds[17].

In this paper, we studied the influence of alternative acceptor groups bis(fluoromesityl) boryl((FMes)$_2$B, FMes= fluoromesityl = 2,4,6-tris(trifluoromethyl) phenyl), which is an analogue of (Mes)$_2$B with the methyl groups replaced by CF$_3$ oxidation groups [18], under different conditions: in vacuum, in the nonpolar solvents Hexane and Toluene, and in the polar solvents THF and CH$_3$CN. By using 3D real-space analysis [19-24], we studied the properties of charge and energy transfer, transition of the dipole moment, electron-hole coherence and delocalization of compounds in different solvents at excited states. From the absorption spectra, emission spectra and analysis of the 3D real-space, we found that significant red shift or blue shift of both absorption maxima and fluorescence maxima of compounds 1-4 in more polar solvents, indicating a strong intramolecular charge transfer (ICT) feature and suggests that the bigger the polarity of the solvent, the greater the shift in red or blue.

2. Theoretical methods

The models in the calculations of compounds 1-4 can be seen in Figure 1. All of the calculations are done using Gaussian 09 software [25], the ground state geometries were optimised using the density functional theory (DFT), B3LYP functional, and 6-31G (d) basis sets, and the excited state electronic properties were calculated using time-dependent DFT (TD-DFT), CAM-B3LYP functional and 6-31G (d) basis sets [26-29].
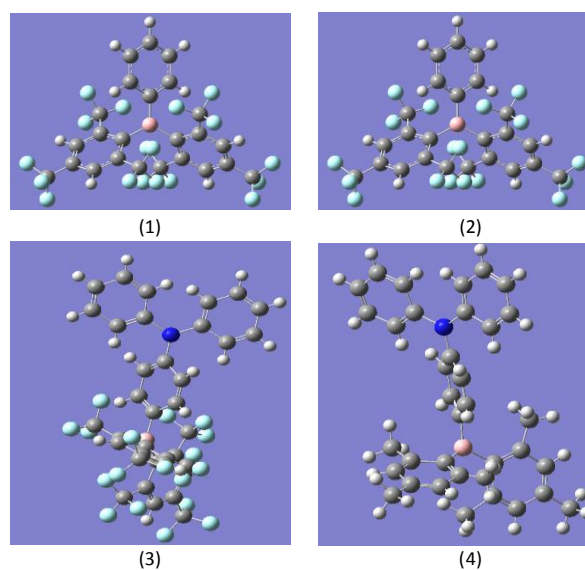
Figure 1: Figures (1), (2), (3), (4) was the model of compound 1, 2, 3 and 4, respectively.

Department of Physics, Liaoning University, Shenyang, China (Y. Ding yding@lnu.edu.cn; J.SH sj566@126.com)

The fluorescence of compounds 1-4 in the visible region were calculated using time-dependent DFT (TD-DFT), CAM-B3LYP functional and 6-31G (d) basis sets. Absorption and fluorescence spectra were obtained using Origin 8. The properties of the excited state was visualised using 3D real space analysis methods [30-33]. In the 3D cube representation, the charge difference density (CDD) shows results of the charge and energy transfer, calculated using [34]

$$\Delta\rho_{\mu,C}(\vec{\gamma}) = \sum_{\substack{a\in unocc \\ i,j=occ}} C_{\mu a j} C_{\mu a j} \varphi_j(\vec{\gamma}) - \sum_{\substack{a,b\in unocc \\ i=occ}} C_{\mu b i} C_{\mu a i} \varphi_b(\vec{\gamma})\varphi_a(\vec{\gamma})$$

,

The first and second terms in the formula code for electron-hole by CDD [35].

3. Results and discussion

3.1 Electronic properties of compounds 1, 2, 3, 4 at ground state

We optimized the ground state geometry of compounds 1-4 using DFT at B3LYP/6-31G (d) level. The highest occupied molecular orbital (HOMO) and the lowest unoccupied molecular orbital (LUMO) [36, 37] are seen under vacuum and in CH_3CN，Hexane，THF and Toluene, respectively (Figure 2). From Figure 2(a), we conclude that different solvents do not significantly affect the orbit of HOMO/LUMO for compound 1. The same analyses were carried out on the compounds 2, 3, 4, with similar conclusions. We can identify that the electron transfers from the lowest unoccupied molecular orbital (LUMO) is mainly an intramolecular charge transfer transition, where the red and green moieties represent the electron and hole [38].
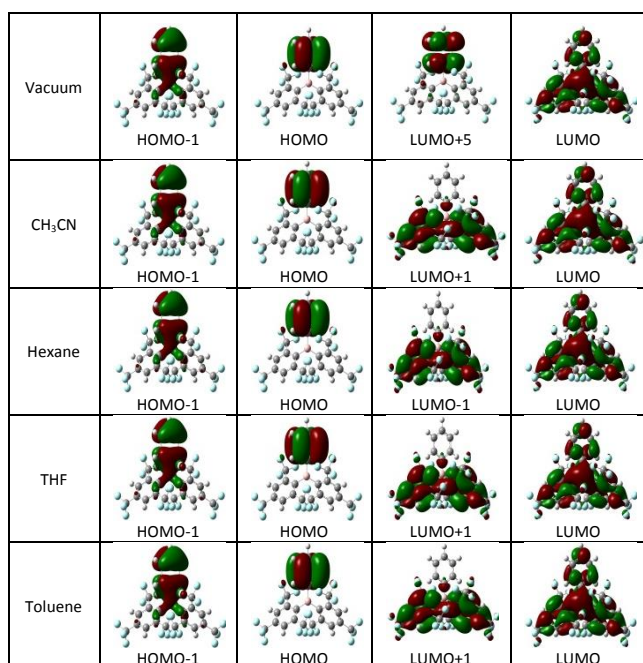
Figure 2(a): 3D Cube of compound 1 on the orbit of HOMO and LUMO
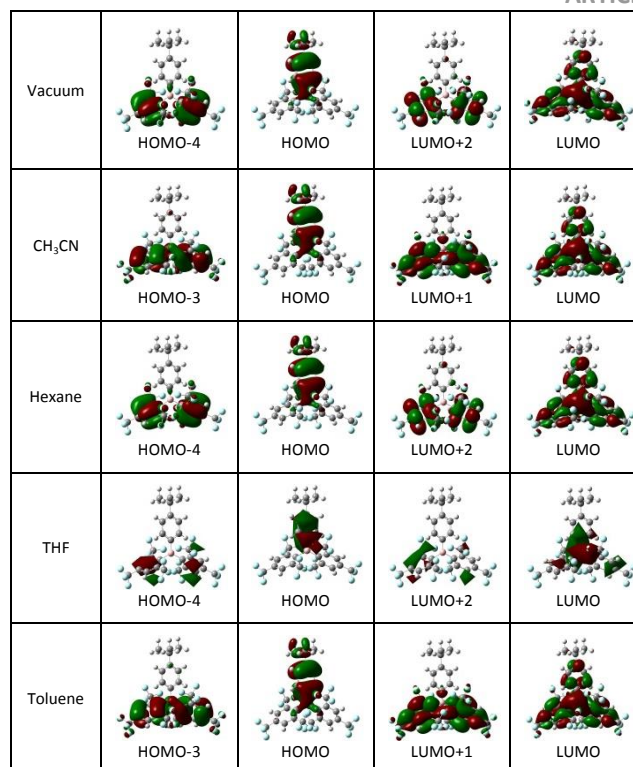
Figure 2(b): 3D Cube of compound 2 on the orbit of HOMO and LUMO
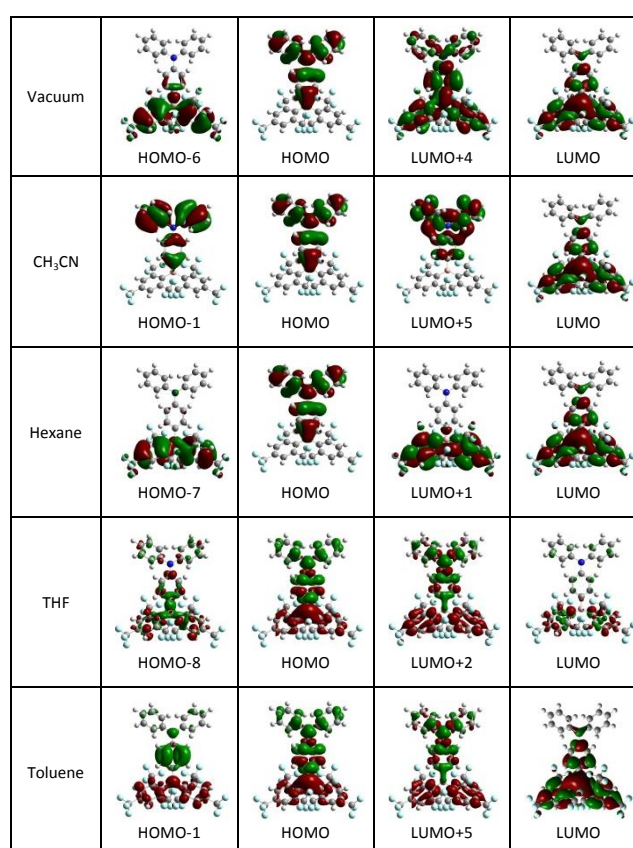
Figure 2(c): 3D Cube of compound 3 on the orbit of HOMO and LUMO

Vacuum	HOMO-3	HOMO	LUMO+6	LUMO
CH$_3$CN	HOMO-1	HOMO	LIMO+3	LUMO
Hexane	HOMO-2	HOMO	LUMO+4	LUMO
THF	HOMO-2	HOMO	LUMO+4	LUMO
Toluene	HOMO-4	HOMO	LUMO+8	LUMO
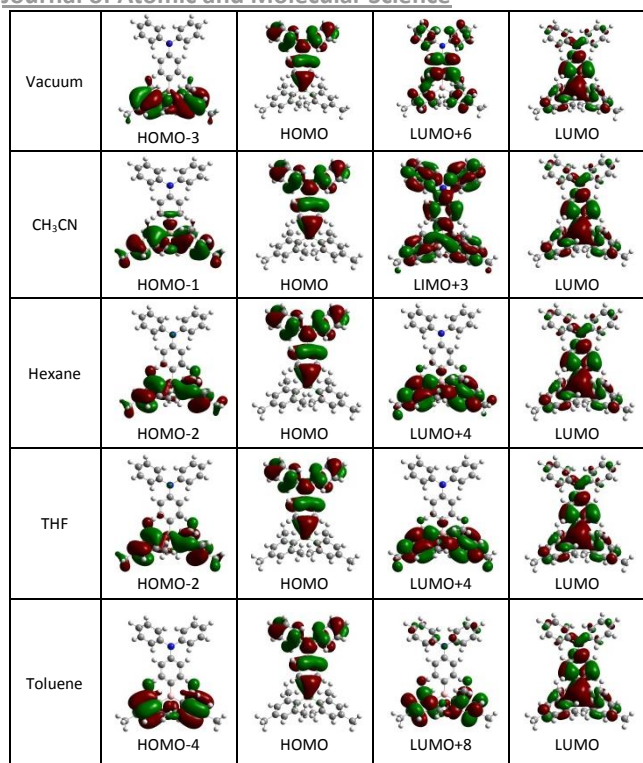
Figure 2(d): 3D Cube of compound 4 on the orbit of HOMO and LUMO

3.2 Excited states properties of compounds 1-4

Photo induced excited state properties of compounds 1-4 were investigated using the TD-DFT method with CAM-B3LYP functional at the 6-31G (d) basis set. The calculated absorption and fluorescence spectra in the visible region can be seen from Figure 3 to Figure 11.

(a) (b)
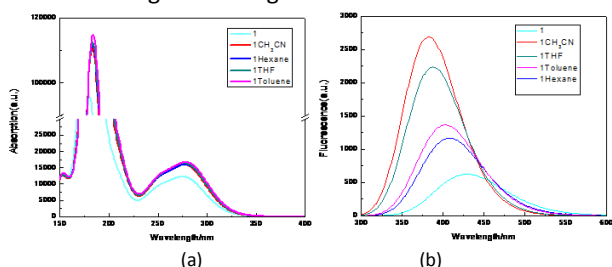
Figure 3: (a) Absorption spectra and (b) fluorescence spectra of compound 1 in vacuum, Hexane, Toluene, THF and CH$_3$CN, respectively.

Figure 3(a) the absorption spectra of compound 1 were slightly red-shifted and only slightly dependent on the polarity of the solvent. Figure 3(b) the varying peaks of the fluorescence spectra of compound 1 provide the evidence that these peaks shifted into the blue when in Hexane, Toluene, THF and CH$_3$CN, compared to in a vacuum. It is notable that the blue shift of the fluorescence spectra of compound 1 in all solvents is significant, the fluorescence maxima of compound 1 is 429.0 nm (2.89 eV) in vacuum, 407.2 nm (3.045 eV) in the nonpolar solvent Hexane, 402.4 nm(3.081 eV) in the nonpolar solvent Toluene, 387.1 nm(3.203 eV) in the polar solvent THF, 382.7 nm(3.240 eV) in the polar solvent CH$_3$CN. It is clear that blue shifted of the

fluorescence maximum of compound 1 is larger in more polar solvents compared to that seen in nonpolar solvents. The largest blue shift of fluorescence is 46.3 nm when compound 1 is in the strongest polar solvent CH$_3$CN. It shows a stronger sensitivity to changes in solvent polarity.

(a) (b)
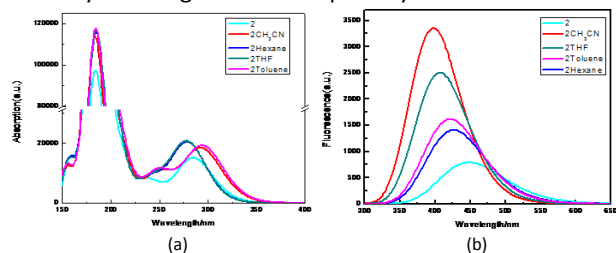
Figure 4: (a) Absorption spectra and (b) fluorescence spectra of compound 2 in Vacuum, Hexane, Toluene, THF and CH$_3$CN, respectively.

Figure 4(a) shows the absorption spectra of compound 2. Compound 2 in CH$_3$CN results in a blue shift, and in Hexane and THF results in a red shift. Figure 4(b) illustrates the fluorescence peaks of compound 2 at 448.6 nm (2.764 eV) in vacuum, 426.2 nm (2.909 eV) in Hexane, 422.0 nm (2.938 eV) in Toluene, 407.2 nm (3.045 eV) in THF, and 397.6 nm (3.118 eV) in CH$_3$CN. It can be concluded that the fluorescence of compound 2 will shift towards blue in all solvents, regardless of their polarity.

(a) (b)
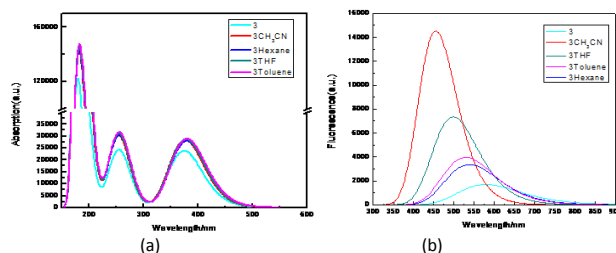
Figure 5: (a) Absorption spectra and (b) fluorescence spectra of compound 3 in vacuum, Hexane, Toluene, THF and CH$_3$CN, respectively.

As seen from Figure 5(a), the calculated absorption spectra of compound 3 is in the visible region and dependent on solvent polarity. The maximum red shift can be observed when the compound 3 is in CH$_3$CN.

Figure 5(b) shows that the fluorescence peaks of compound 3 at 578.4 nm (2.144 eV) in vacuum, 536.8 nm (2.31 eV) in Hexane, 530.0 nm (2.339 eV) in Toluene, 498.6 nm (2.487 eV) in THF, and 454.2 nm(2.73 eV) in CH$_3$CN. This is a blue shift in all solvents.
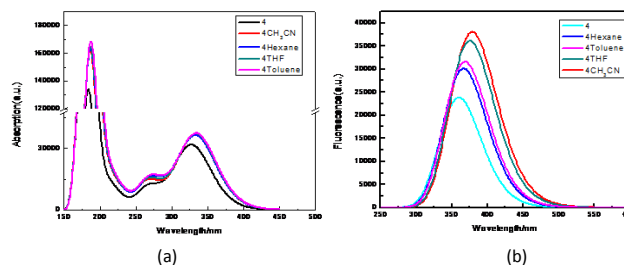
(a) (b)

Figure 6: (a) Absorption spectra and (b) fluorescence spectra of compound 4 in vacuum, Hexane, Toluene, THF and CH$_3$CN, respectively.

Figure 6(a) shows the absorption spectra of compound 4 in all solvents. It is notable that the absorption maxima of compound 4 in all solvents is a red shift. Figure 6(b) illustrates the fluorescence peaks of compound 4 at 359.7 nm (3.447 eV) in vacuum, 366.9 nm (3.379 eV) in Hexane, 369.0 nm (3.360 eV) in Toluene, 375.0 nm (3.306 eV) in THF, and 378.3 nm (3.277 eV) in CH₃CN. The fluorescence spectra indicates that the fluorescence peaks are shifted towards red.
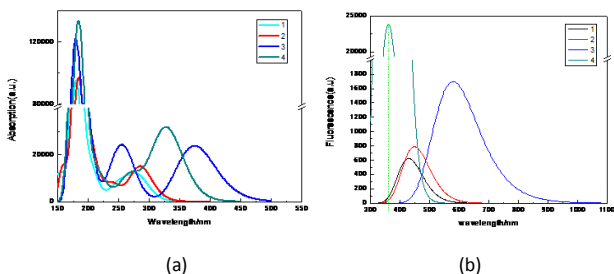

Figure 7: (**a**) Absorption spectra and (**b**) fluorescence spectra of compound 1-4 in vacuum, respectively.

Figure 7(a) shows the absorption spectra of compounds 1-4 in vacuum with absorption peaks at 180.2 nm (6.88 eV), 184.4 nm (6.723 eV), 179 nm (6.926 eV), 183.6 nm (6.753 eV), respectively. Compared to compound 1, which has an absorption peak at 180.2 nm (6.880 eV), compound 2 and 4 show a red shift of 4.2 nm and 3.4 nm. Compound 3 shows a blue shift of 1.2 nm. To gather more information of the red shift of compounds 1-4 in vacuum, we studied the absorption spectra of compound 2. The dramatic blue shift of compound 3 makes this compound a good one to study for more information about blue shift of the compounds. Figure 7(b) shows the fluorescence spectra of compounds 1-4 in vacuum. Fluorescence peaks are seen at 429.0 nm (2.890 eV), 448.6 nm (2.764 eV), 578.4 nm (2.144 eV), 359.7 nm (3.447 eV), respectively. Compared to compound 1, compounds 2 and 3 display a red shift of 19.6 nm and 149.4 nm. Compound 3 is has a red shift and compound 4 shows a blue shift of 69.3 nm.
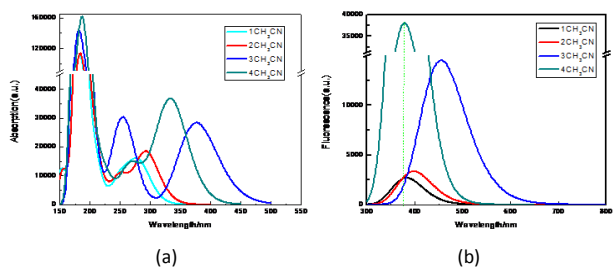
Figure 8: (**a**) Absorption spectra and (**b**) fluorescence spectra of compound 1-4 in CH₃CN, respectively.

As seen in Figure 8(a), absorption maxima of compounds 1, 2, 3 and 4 are at 183.0 nm (6.775 eV), 183.7 nm (6.749 eV), 182.0 nm (6.812 eV), 186.8 nm (6.637 eV), respectively, in the polar solvent CH₃CN. We also investigated the compounds in other solvents, e.g. Figure 8(b) showing fluorescence peaks at 382.7 nm (3.24.0 eV), 397.6 nm (3.118 eV), 454.2 nm (2.73.0 eV), 378.3 nm (3.277 eV) in CH₃CN, Figure 9(a) and 9(b) displaying the absorption maxima at 183.0 nm (6.775 eV),

184.4 nm (6.723 eV), 182.0 nm (6.812 eV), 186.8 nm (6.637 eV) and fluorescence peaks at 407.2 nm (3.045 eV), 426.2 nm (2.909 eV), 536.8 nm (2.31.0 eV), 366.9 nm (3.379 eV) of compounds 1, 2, 3 and 4, respectively, in the nonpolar solvent Hexane, Figure 10(a) and 10(b) shows absorption peaks at 183.0 nm (6.775 eV), 184.4 nm (6.723 eV), 182.0 nm (6.812 eV), 186.8 nm (6.637 eV) and fluorescence peaks at 387.1 nm (6.637 eV), 407.2 nm (3.045 eV), 498.6 nm (2.487 eV), 375.0 nm (3.306 eV) of compounds 1, 2, 3 and 4, respectively, in the polar solvent THF and Figure 11(a) and 11(b) shows absorption peaks at 183.7 nm (6.749 eV), 184.4 nm (6.723 eV), 182.6 nm (6.79 eV), 187.6 nm (6.609 eV) and fluorescence emission peaks at 402.4 nm (3.081 eV), 422.0 nm (2.938 eV), 530.0 nm (2.339 eV), 369.0 nm (3.36.0 eV) for compounds 1, 2, 3 and 4, respectively, in the nonpolar solvent Toluene.

On the basis of the above results, it can be seen that absorption peaks of compounds 1-4 are slightly different (Figure 8(a), Figure 9(a), Figure 10(a) and Figure 11(a)), and the absorption spectra depend a little bit on the polarity of the solvent (Figure 8(b), Figure 9(b), Figure 10(b) and Figure 11 (b)).
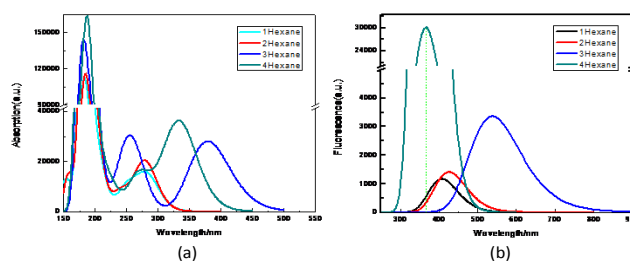
Figure 9: (a) Absorption spectra and (b) fluorescence spectra of compounds 1-4 in Hexane, respectively.
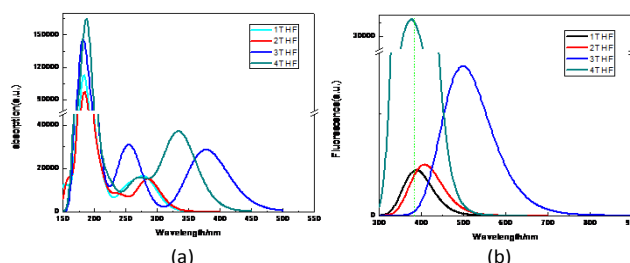
Figure 10: (a) Absorption spectra and (b) fluorescence spectra of compounds 1-4 in THF, respectively.
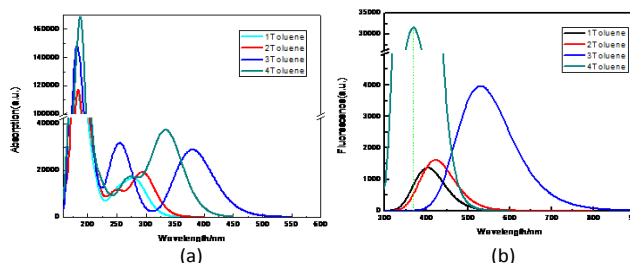
Figure 11: (**a**) Absorption spectra and (**b**) fluorescence spectra of compounds 1-4 in Toluene, respectively

3.3 3D cube representations of compounds 1-4

The analysis of 3D real space was employed to study the properties of excited states of the compounds 1-4. The electronic transition and molecular orbits are shown in Figure 12, where the red and green moieties represent the electrons and holes. From Figure 12(a), we can clearly identify that the electron transfers from top to bottom in the S_1 excited state of compound 1 in different solvents. This is an intramolecular transition and the corresponding electron transfer is mainly formed by a HOMO-1 to LUMO transition. From Figure 12(a), at S_3 excited state of compound 1 in different solvents suggests that the orbital transition is from HOMO-2 to LUMO. The analysis of the electron transfer indicates at the S_1 excited state of compound 1 are mainly formed by HOMO-1 to LUMO transition.
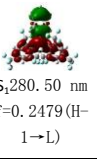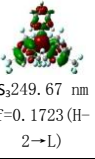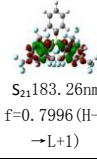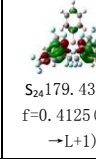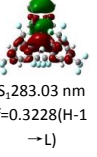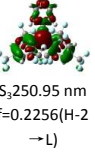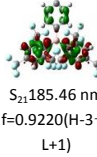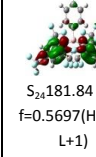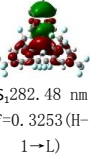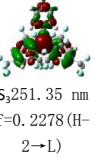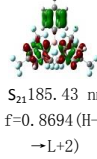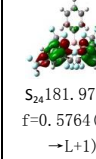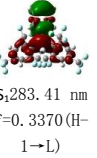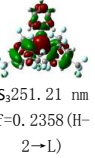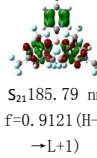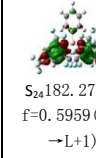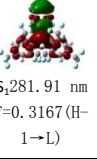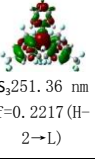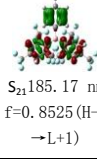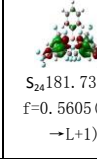
Vacuum	$S_1$280.50 nm f=0.2479 (H−1→L)	$S_3$249.67 nm f=0.1723 (H−2→L)	S_{21}183.26nm f=0.7996 (H−3→L+1)	S_{24}179.43 nm f=0.4125 (H−4→L+1)
Hexane	$S_1$283.03 nm f=0.3228(H−1→L)	$S_3$250.95 nm f=0.2256(H−2→L)	S_{21}185.46nm f=0.9220(H−3→L+1)	S_{24}181.84 nm f=0.5697(H−4→L+1)
THF	$S_1$282.48 nm f=0.3253(H−1→L)	$S_3$251.35 nm f=0.2278 (H−2→L)	S_{21}185.43 nm f=0.8694 (H−4→L+2)	S_{24}181.97 nm f=0.5764 (H−4→L+1)
Toluene	$S_1$283.41 nm f=0.3370(H−1→L)	$S_3$251.21 nm f=0.2358 (H−2→L)	S_{21}185.79 nm f=0.9121 (H−3→L+1)	S_{24}182.27 nm f=0.5959 (H−4→L+1)
CH$_3$CN	$S_1$281.91 nm f=0.3167 (H−1→L)	$S_3$251.36 nm f=0.2217 (H−2→L)	S_{21}185.17 nm f=0.8525 (H−3→L+1)	S_{24}181.73 nm f=0.5605 (H−4→L+1)

Figure12: (**a**) The 3D Cube of compound 1 with large oscillator strength correspond to S1, S3 , S21, S24 states, respectively.

The analysis the 3D real space of the S_3 excited state of compound 1 indicates that the electron transfer is primarily by an intramolecular charge transfer HOMO-2 to LUMO in all solvents.

The analysis of the 3D real space of S_{21} excited state of compound 1 primarily formed by HOMO-3 to LUMO+1, indicated that the electron transfer was primarily by an intramolecular charge transfer under the top boron-bonded phenyl ring. Compared to the 3D real space of the S_{21} excited state of compound 1 in vacuum, the 3D real space in CH$_3$CN, Hexane, THF,

Toluene indicates there is a strong donor from the top boron-bonded phenyl ring. The analysis of the 3D real space of the S_{24} excited state of compound 1 are primarily formed by HOMO-4 to LUMO+1 electron transfer, which is an intramolecular charge transfer independent of the solvent. The same analysis was carried out on the 3D real space of compounds 2, 3 and 4 with large oscillator strengths (Figures 12(b), (c) and (d), respectively).
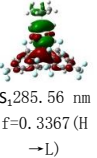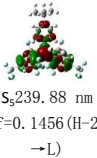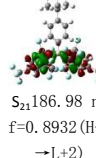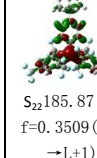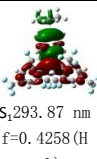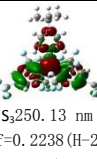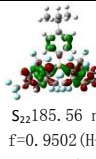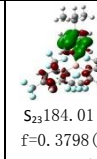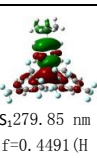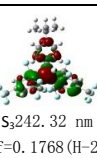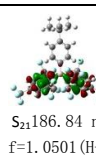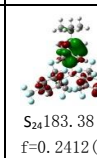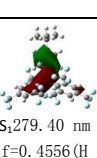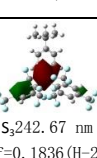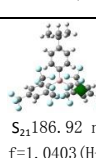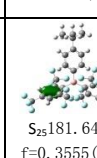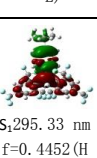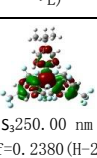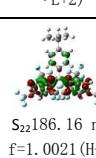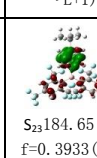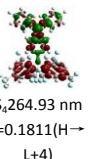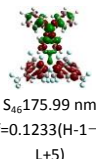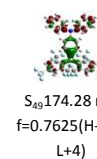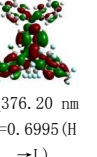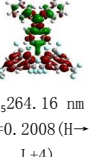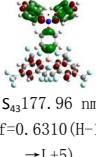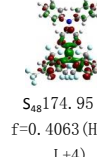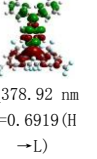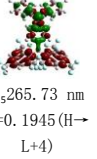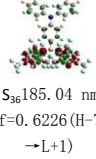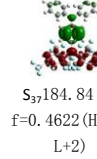
Vacuum	$S_1$285.56 nm f=0.3367 (H→L)	$S_5$239.88 nm f=0.1456 (H−2→L)	S_{21}186.98 nm f=0.8932 (H−4→L+2)	S_{22}185.87 nm f=0.3509 (H−4→L+1)
CH$_3$CN	$S_1$293.87 nm f=0.4258 (H→L)	$S_3$250.13 nm f=0.2238 (H−2→L)	S_{22}185.56 nm f=0.9502 (H−3→L+1)	S_{23}184.01 nm f=0.3798 (H−1→L+5)
Hexane	$S_1$279.85 nm f=0.4491 (H→L)	$S_3$242.32 nm f=0.1768 (H−2→L)	S_{21}186.84 nm f=1.0501 (H−4→L+2)	S_{24}183.38 nm f=0.2412 (H−1→L+4)
THF	$S_1$279.40 nm f=0.4556 (H→L)	$S_3$242.67 nm f=0.1836 (H−2→L)	S_{21}186.92 nm f=1.0403 (H−4→L+2)	S_{25}181.64nm f=0.3555 (H−5→L+1)
Toluene	$S_1$295.33 nm f=0.4452 (H→L)	$S_3$250.00 nm f=0.2380 (H−2→L)	S_{22}186.16 nm f=1.0021 (H−3→L+1)	S_{23}184.65 nm f=0.3933 (H→L+5)

Figure 12: (**b**) The 3D Cube of compound 2 with large oscillator strength.

Vacuum	$S_1$374.14 nm f=0.5865(H→L)	$S_4$264.93 nm f=0.1811(H→L+4)	S_{46}175.99 nm f=0.1233(H−1→L+5)	S_{49}174.28 nm f=0.7625(H−6→L+4)
CH$_3$CN	$S_1$376.20 nm f=0.6995 (H→L)	$S_5$264.16 nm f=0.2008 (H→L+4)	S_{43}177.96 nm f=0.6310 (H−1→L+5)	S_{48}174.95 nm f=0.4063 (H−6→L+4)
Hexane	$S_1$378.92 nm f=0.6919 (H→L)	$S_5$265.73 nm f=0.1945 (H→L+4)	S_{36}185.04 nm f=0.6226 (H−7→L+1)	S_{37}184.84 nm f=0.4622 (H−2→L+2)
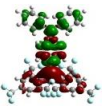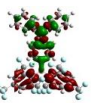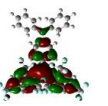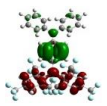
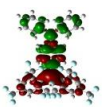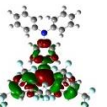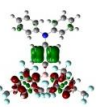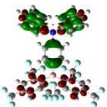|				
THF	S_1 377.41 nm f=0.7064 (H→L)	S_5 264.69 nm f=0.2002 (H→L+4)	S_{36} 184.82 nm f=0.3925 (H-8→L+2)	S_{37} 184.51 nm f=0.3730 (H-2→L+2)
Toluene	S_1 379.56 nm f=0.7115 (H→L)	S_9 245.88 nm f=0.2832 (H-6→L)	S_{36} 185.25 nm f=0.5449 (H-7→L+1)	S_{43} 178.25 nm f=0.6535 (H-1→L+5)

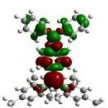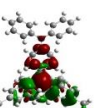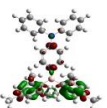**Figure 12**: (**c**) The 3D Cube of compound 3 with large oscillator strength.
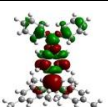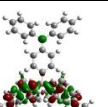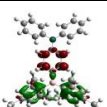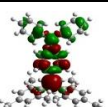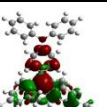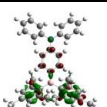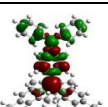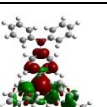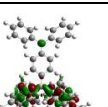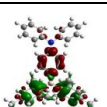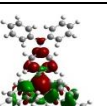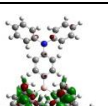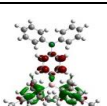
Vacuum	S_1 329.52 nm f=0.7336 (H→L)	S_2 298.73 nm f=0.1113 (H-1→L)	S_{33} 185.33 nm f=0.6722 (H-3→L+6)	S_{35} 184.11 nm f=0.4168 (H-4→L+4)
CH$_3$CN	S_1 334.67 nm f=0.8756 (H→L)	S_2 295.47 nm f=0.1307 (H-1→L)	S_{29} 189.33 nm f=0.7912 (H-2→L+4)	S_{33} 186.52 nm f=0.4178 (H-4→L+4)
Hexane	S_1 335.07 nm f=0.8527 (H→L)	S_2 298.41 nm f=0.1454 (H-1→L)	S_{30} 189.12 nm f=0.9754 (H-2→L+4)	S_{33} 186.52 nm f=0.4727 (H-4→L+4)
THF	S_1 335.16 nm f=0.8807 (H→L)	S_2 296.20 nm f=0.1358 (H-1→L)	S_{29} 189.55 nm f=0.9398 (H-2→L+4)	S_{30} 188.91 nm f=0.2736 (H-1→L+3)
Toluene	S_1 335.99 nm f=0.8788 (H→L)	S_2 298.13 nm f=0.1484 (H-1→L)	S_{29} 189.77 nm f=1.1274 (H-4→L+8)	S_{33} 186.95 nm f=0.4688 (H-4→L+4)

Figure 12: (**d**) The 3D Cube of compound 4 with large oscillator strength

4. Conclusionss

In this work, we have investigated the absorption and fluorescence spectra of 4 compounds with an aryl ring directly bound to a (FMes) 2B group through B-C bonds in vacuum, in the nonpolar solvents Hexane and Toluene, and in the polar solvents THF and CH$_3$CN. We found the same trends in red or blue shift in different solvents across all 4 compounds (Figures 7- 11). There is significant red or blue shift of both absorption and fluorescence maxima of compounds 1-4 in more polar solvents, indicating a strong intramolecular charge transfer capacity. We suggest that the stronger the polarity of the solvent, the greater the red or blue shift. 3D cube representations of compounds 1-4 in the four main excited states and the corresponding orbital transitions are presented.

Acknowledgements

References

[1] Z. Yuan, N. J. Taylor, Y. Sun, T. B. Marder, L. D. Williams and C. Lap -Tak, Chem., 449 (1993) 27-37.
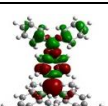
[2] Z. Yuan, N. J. Taylor, R. Ramachandran and T. B. Marder, Chem., 10 (1996) 305-316.

[3] Z. Yuan, J. C. Collingsb, N.J. Taylora and T.B. Mardera, J. Solid State Chem., 154 (2000) 5-12.

[4] Z. Yuan, C. D. Entwistle, J. C. Collings, D. Albesa-Jove, A. S. Batsanov, J. A. K. Howard, N. J. Taylor, H. M. Kaiser, D. E. Kaufmann, S. Y. Poon, W. Y. Wong, C. Jardin, S. Fathallah, A. Boucekkine, J. F. Halet and T. B. Marder, Chem.Eur. J., 12 (2006) 2758-2771.

[5] M. Charlot, L. Porrès, C. D. Entwistle, A. Beeby, T. B. Marder and M. Blanchard-Desce, Phys. Chem. Chem. Phys., 4600 (2005) 606.

[6] J. C. Collings, S.Y. Poon, C. L. Droumaguet, M. Charlot, C. Katan, L. O. Pålsson, A. Beeby, J. A. Mosely, H. M. Kaiser, D. Kaufmann, W. Y. Wong, M. Blanchard-Desce and T. B. Marder, Chem.Eur. J., 15 (2009) 198-208.

[7] L. Ji, R. M. Edkins, L. J. Sewell, A. Beeby, A. S. Batsanov, K. Fucke, M. Drafz, J. A. K. Howard, O. Moutounet, F. Ibersiene, A. Bouceckine, E. Furet, Z. Liu, J.-F. Halet, C. Katan and T. B. Marder, Chem.Eur. J., 20 (2014) 13618-13635.

[8] Z. Liu, T. Chen, B. Liu, Z.-L. Huang, T. Huang, S. Li, Y. Xu and J. Qin, J. Mater. Chem., 17 (2007) 4685-4689.

[9] A. Karotki, M. Drobizhev, M. Kruk, C. Spangler, E. Nickel, N. Mamardashvili and A. Rebane, J. Opt. Soc. Am. B., 20 (2003) 321-332.

[10] G. Wittig and W. Herwig, Chem .Ber., 88 (1955) 962-976.

[11] J.C. Doty, B. Babb, P.J. Grisdale ,M. Glogowski, J.L. Williams and R.J .Organomet, Chem., 38 (1972) 229-236.

[12] Y. Sun, N. Ross, S.-B. Zhao, K. Huszarik, W.-L. Jia, R.-Y. Wang, D. Macartney and S. Wang, J. Am. Chem. Soc., 129 (2007) 7510-7511.

[13] A. Sundararaman, K. Venkatasubbaiah, M. Victor,L. N. Zakharov, A. L. Rheingold and F. Jakle, J. Am. Chem. Soc., 128 (2006) 16554-16565.

[14] A. Sundararaman,R. Varughese, H. Li, L. N. Zakharov, A. L. Rheingold and F. Jakle, Organometallics, 26 (2007) 6126-6131.

[15] H. Braunschweig, A. Damme, J. O. C. Jimenez-Halla, C. Horl, I. Krummenacher, T. Kupfer, L. Mailander and K. Radacki, J. Am. Chem. Soc., 134 (2012) 20169-20177.

[16] A. E. Ashley, T. J. Herrington, G. G. Wildgoose, H. Zaher, A. L. Thompson, N. H. Rees, T. Kramer and D. O'Hare, J. Am. Chem. Soc., 133 (2011) 14727-14740.

[17] Z. l. Zhang, R. M. Edkins, J. Nitsch, K. Fucke, A. Steffen, L. E. Longobardi, D. W. Stephan, C. Lambertd and T. B. Marder*, Chem. Sci., 6 (2015) 308-321.

[18] L. Weber, V. Werner, M. Fox, T. B. Marder, S. Schwedler, A. Brockhinke, H.-G. Stammler and B. Neumann, Dalton Trans., 8 (2009) 1339-1351.

[19] W. J. D. Beenken and T. Pullerits, Journal of Physical Chemistry B, 108 (2004) 6164-6169.

[20] S. Tretiak, A. Saxena, R. L. Martin, and A. R. Bishop, Physical Review Letters, 89 (2002) 974021 – 974024.

[21] Y.Z. Li, F.C. Ma, B. Dong, J. Li, and M.D. Chen, Dyes and Pigments, 92 (2012) 1344-1350.

[22] S. Mukamel, S. Tretiak, T. Wagersreiter, et al, Science, 277 (1997) 781-787.

[23] Y.L. Chu and Z. Yang, Chin. J. Chem. Phys., 25 (2012) 654-658.

[24] M. T. Sun, P. Song, Y. H. Chen et al, Chem. Phys. Lett., 416 (2005) 94-99.

[25] P. Song and F. C. Ma, J. Phys. Chem. A., 114 (2010) 2230-2234.

[26] P. J .Hay and W. R. Wadt, J. Chem. Phys., 82 (1985) 270.

[27] E. K. U. Gross and W. Kohn, Phys. Rev. Lett. 55 (1985) 2850.

[28] A. D. Becke, Phys. Rev. A: At., Mol., Opt. Phys., 38 (1988) 3098.

[29] C. Lee, W. Yang and R. G. Parr, Phys. Rev. B. ,37 (1988) 785.

[30] L. C. Zhou, G. J. Zhao, J. F. Liu, Y. K. Wu, X. J. Peng and M. T. Sun, J. Photochem. Photobiol., A187 (2007) 305.

[31] M. T. Sun, J. Chem. Phys., 124 (2006) 054903.

[32] S. Mukamel, S. Tretiak, T. Wagersreiter and V. Chernyak, Sci., 277(1997) 781.

[33] M. T. Sun, Y. Ding and H. X. Xu, J. Phys. Chem., B111 (2007) 13266.

[34] W. J. D. Beenken and T. Pullerits, J. Phys. Chem., B108 (2004), 6164.

[35] M. T. Sun, Chem Phys Letts. 408 (2005) 128.

[36] L. C. Zhou, G. J. Zhao, J. F. Liu, Y. K. Wu, X. J. Peng and M. T. Sun, J. Photochem. Photobiol. A187 (2007), 305.

[37] J. Liu, J. Xia, ChemPhysChem., 15(2014)2626-2633.

[38] X. Zhang, L. Guo and Y.B. Jiang, Acta Phys. Chim. Sin., 20 (2004) 930-935.